Construction and Building Materials 278 (2021) 122414

Contents lists available at ScienceDirect

Construction and Building Materials

journal homepage: www.elsevier.com/locate/conbuildmat

Systematic evaluation of the aggregate types and properties on metakaolin based geopolymer composites

Furkan Şahin [a,*], Mucteba Uysal [b], Orhan Canpolat [b]

[a] Istanbul University-Cerrahpasa, Civil Engineering Department, Avcilar Campus, Istanbul, Turkey
[b] Yildiz Technical University, Civil Engineering Department, Davutpasa Campus, Istanbul, Turkey

HIGHLIGHTS

- Metakaolin can be used with different fillers for geopolymer production.
- The highest results were yielded with basalt sand for geopolymer mortar.
- Acceptable results were obtained with the waste concrete aggregate.
- The geopolymer composites resisted the elevated temperatures.

ARTICLE INFO

Article history:
Received 25 October 2020
Received in revised form 9 January 2021
Accepted 12 January 2021
Available online 4 February 2021

Keywords:
Geopolymer
Metakaolin
Waste concrete aggregate
Basalt sand
Silica sand
Sandstone
High temperature
Freezing-thawing

ABSTRACT

Although aggregates constitute the largest volume in geopolymer composites, there are limited studies related to this parameter. This study investigates the effect of different types of aggregates on the mechanical and durability properties of metakaolin (MK) based geopolymer composites. For this study, while using metakaolin as the main raw material, slag (S) was used to gain an early setting. Six different sand types (silica sand, river sand, sandstone, Rilem sand, waste concrete aggregate, and basalt sand) were used in the geopolymer mortar. The ultrasonic pulse velocity (UPV) and flexural and compressive strength results of 7, 28, and 56 days were found to examine the effect of aggregates, while the unit weight, voids ratio, water absorption, and workability properties of the samples were also investigated. XRD analyzes were performed for the crystalline materials' structure. After 56 days, the samples were exposed to 180 cycles of the freezing-thawing test (1 cycle consists of 12 h at −18 °C and 12 h at +4 °C) and high temperatures of 200, 400, 600, and 800 °C. After the tests, UPV and strength results were found and weight changes were also examined. Also, an abrasion test was applied. SEM analyzes were carried out pre and post the high-temperature test. Test results have shown that basalt sand added samples produced better results due to their more dense and compact structure compared to other aggregates. Similarly, high results were obtained by using silica sand and sandstone. In the case of using waste concrete aggregate, it was seen that acceptable results were obtained in terms of structural features.

© 2021 Elsevier Ltd. All rights reserved.

1. Introduction

Geopolymer composite products are accepted as an alternative to Portland cement products by large segments today. The main raw material of geopolymer products is aluminosilicates. Aluminosilicate raw materials are converted into products by the geosynthetic method. These three-dimensional amorphous products were first named as "geopolymer" by Davidovits in 1978 [1]. Clay minerals and calcined clays have an important place among the materials used for the synthesis of geopolymer products. Geopolymer products are produced by the alkali activation of such aluminosilicates. Produced by activating the kaolin with a high-temperature effect in the 600–900 °C range, metakaolin is an easily available and low-cost geopolymer precursor binder material [2]. Kaolin clay is one of the important aluminosilicates in the earth's crust [3]. Metakaolin, produced by calcining kaolin, is a reactive binder material that contains highly amorphous phases that are easily involved in the geopolymerization reaction. Metakaolin is a popular material because it contains a more stable chemical composition and fewer impurities than waste main binder materials

* Corresponding author.
E-mail address: furkansahintr@gmail.com (F. Şahin).

https://doi.org/10.1016/j.conbuildmat.2021.122414
0950-0618/© 2021 Elsevier Ltd. All rights reserved.

such as fly ash and blast furnace slag that have the potential to be used in this field [4].

There are limited studies about the use of different sands as aggregates in the geopolymer mortar. An important of these is waste concrete. Waste concrete is obtained from structures such as collapsed buildings, bridges, pavements [5]. It is possible to evaluate the waste concrete obtained in this way as important source material to reduce the consumption of natural aggregates from non-renewable materials [6–8]. Despite this situation, the porous structure of the old cement mortar attached to the surface of the recycled concrete aggregate plays an important role in mechanical properties [9]. Etxeberria et al. [10] used recycled concrete aggregates in Portland cement concrete and saw a decline in strength results. Similar results were also identified by Sagoe-Crentsil et al. [11] and Tabsh and Abdelfatah [12]. Also, it has been observed that waste concrete increased water absorption and drying shrinkage by 50% [13]. The main reasons for this situation were lower density in old cement mortar, high water absorption capacity, and a high rate of available impurities [14–16]. Although there are dısadvantages, the evaluating of used concretes as recycling is also an important step towards increasing the sustainability of concrete that completes its life by reducing the condition of transporting and stacking concrete wastes to landfills. Thus it also helps to protect soil fill areas. It is a strategic alternative resource especially for developing countries that have aggregate resource problems [17,18].

It is very common to use limestone aggregates in concrete and mortar production. Basaltic rock aggregates have a structure similar to limestone aggregates. Basalt is a hard, dense volcanic igneous rock that is widely available worldwide. Igneous minerals are mostly active today and are converted into clay minerals with a stable structure by chemical and physical decomposition [19]. Basalt has long been used in architectural applications such as tiles and slab construction. Also, cast basalt liners used in steel pipe production show superior abrasion resistance in different industrial applications. It is also possible to evaluate crushed basalts as aggregates. Crushed basalt aggregates are fine-grained rocks formed by rising solidification of molten lava found deep in the Earth's crust, close to dark green and black [20]. It is frequently used in airport and highway pavement construction. There are also studies on the evaluation of basalt powder as a mineral additive [21–23]. It provides superior properties to concrete and mortars. It creates high abrasion resistance and UV resistance and a tight grain structure. Also, it increases the specific gravity value while lowering the absorption and abrasion loss values [24]. It has been observed that it is appropriate to use basalt in concrete and mortar structure within the framework of examined cases.

Silica sand is a byproduct obtained in the wet process of cement production. It has the potential to be used as a substitute for fine aggregate and has the properties of reducing pores and better moisture resistance. The use of silica sand in concrete and mortars reduces the cost while increasing the strength to a certain extent. Sudhahar et al. [25] achieved a 15.5% increase in concrete and mortars while replacing silica sand with a 50% fine aggregate. Vishnumanohar et al. [26] used silica sand up to 60% instead of fine aggregate in concrete and achieved 15% increases in strength results. Sandstone is a sedimentary rock type consisting of silt-sized particles and rock grains. There is a high rate of feldspar and quartz in sandstones. Sandstones with different types based on geological properties are widely used as aggregates in concrete [27,28]. The high use of river sand in the construction industry has led to depletion and exploitation of natural sand. It also causes environmental problems, such as lowering the water table and sliding of river shores. This triggered the definition of alternative aggregates to river sand [29].

High temperature and freezing-thawing resistance are important features in mortars. There are studies on these subjects. Zhang et al. [30] prepared geopolymer mortars using metakaolin and fly ash and exposed them to high-temperature effects. A geopolymer product was revealed by examining the test results. Duan et al. [31] studied the substitution of silica fume in fly ash-based geopolymer composites and explored the effects created by exposing the formed products to thermal cycles. The residual compressive strengths, weight losses, and microstructural changes as a result of the 7, 28, and 56 heating and cooling cycles have been investigated. Three different temperatures (200, 400, and 800 °C) were performed. An increase in the results was observed with the replacement of silica fume. Celik et al. [32] added four different fibers to the geopolymer mortars prepared using metakaolin and colemanite. They used polyvinyl alcohol, polyolefin, modified polyamide, and basalt fibers as synthetic fibers. When geopolymer mortars were exposed to the effects of 300, 600, and 900 °C, it was determined that the geopolymer mortars maintained their stability even at 900 °C. However, for the freezing-thawing effect, Cai et al. [33] produced geopolymer concrete by using slag. When the freezing-thawing test results were examined, it was seen that a high resistance was formed and the resistance coefficient was close to 90%. Yunsheng et al. [34] showed that when applied 20 cycles for the freezing-thawing test, polyvinyl alcohol-reinforced geopolymer samples did not show a significant effect in terms of hardness and impact resistance. As can be seen, the effects of using binder materials on these tests were generally investigated. Studies on how much these two tests are affected by the aggregate used in geopolymer samples are limited.

There are many studies on metakaolin based geopolymer composite production. Studies have generally investigated the situations in which different binders are replaced with metakaolin. In this study, the effects formed by using six different sand types were investigated, unlike other studies. The study investigating the effect of Rilem sand, waste concrete sand, river sand, sandstone, silica sand, and basalt sand together in geopolymer mortars, is not available in the literature. The results of 7, 28, and 56 days of compressive and flexural strength, UPV values and unit weight, water absorption, voids ratio, and workability were investigated. The produced samples were also subjected to abrasion, high-temperature, and freezing-thawing test. Four different temperatures, 200, 400, 600, and 800 °C, were applied for the high-temperature test. 180 cycles were applied for the freezing-thawing test, one cycle was 12 h at −18 °C and 12 h at +4 °C. UPV, weight changes, and strength results were found before and after the freezing-thawing and high-temperature tests. SEM and XRD were performed for microstructure analysis.

2. Experimental procedure

In the production of geopolymer samples, metakaolin was used as a raw material. Metakaolin is a material with high pozzolanic activity since Al_2O_3 + Fe_2O_3 + SiO_2 content is 97.2%. The thinness of the grain structure helps to accelerate geopolymerization. Blast furnace slag was also added to the mixture. The chemical compositions of metakaolin and blast furnace slag are given in Table 1.

Sodium hydroxide with 12 M and sodium silicate with SiO_2/Na_2O = 3.29 were mixed to prepare an activator mixture. Six different types were used in this study as an aggregate. The first of these is Rilem sand which is in accordance with BS EN 196-1. Along with Rilem sand, waste concrete sand, river sand, sandstone, silica sand, and basalt sand were used in this study. The chemical compositions and physical properties of the aggregates are given in Tables 2 and 3.

Table 1
Chemical composition of the raw materials.

Chemical properties %	SiO_2	Al_2O_3	Fe_2O_3	TiO_2	CaO	MgO	K_2O	Na_2O	L.O.I.
Slag	40.60	12.83	1.37	0.75	36.08	6.87	0.68	0.79	0.03
Metakaolin	56.10	40.25	0.85	0.55	0.19	0.16	0.55	0.24	1.11

Table 2
Chemical composition of the aggregates.

Chemical properties %	SiO_2	Al_2O_3	Fe_2O_3	TiO_2	CaO	MgO	K_2O	Na_2O	L.O.I.
Silica sand	98.80	0.35	0.04	0.10	0.02	0.02	0.15	0.28	0.24
Riversand	73.10	12.20	1.00	0.18	9.30	2.40	0.22	0.67	0.93
Sandstone	44.5	6.2	3.03	0.9	40.2	1.2	1.9	1.12	0.95
Waste concrete sand	60.56	0.52	5.82	0.75	12.01	1.83	1.30	2.69	14.52
Basalt sand	57.9	17.6	8.1	0.9	7.0	2.3	1.9	3.9	0.4
Rilem sand	97.22	nd	nd	nd	1.34	nd	nd	nd	1.44

Table 3
Physical properties of the aggregates.

	Specific gravity	Absorption (%)	Abrasion (%)	Specific surface Area/m^2/kg
Silica sand	2.84	1.67	21	224
Riversand	2.67	1.96	28	208
Sandstone	2.83	1.70	23	220
Waste concrete sand	2.46	2.41	36	180
Basalt sand	2.86	1.60	18	232
Rilem sand	2.64	2.01	30	203

Sodium hydroxide was prepared as 12 M for the activator 24 h before the mixing day. With this situation, the prepared sodium hydroxide was allowed to cool at room conditions. When the mixture was made, the prepared sodium hydroxide solution was blended with sodium silicate as a ratio of 1/2. Then, metakaolin was mixed with the activator mixture as a raw material as a ratio of 1/1. Blast furnace slag was then added by 13% of the binder material (metakaolin) weight for increasing the calcium content and reducing the setting time. In other words, slag was not mixed with the activator mixture in conjunction with metakaolin. First, metakaolin fully reacted with the activator mixture, then the reaction was accelerated by the addition of slag. As aggregate, six different aggregates were added separately, 2.25 times the binder material. Rilem sand, recycled waste concrete sand, river sand, sandstone, silica sand, and basalt sand were used separately. Mixtures used in the preparation of the geopolymer mixture for 450 g binder material are shown in Table 4. Then, the prepared mortars were placed in the molds and exposed to vibration. A stirrer drill was used in the preparation of the mixture.

The samples were removed from the mold after two hours and left in the room conditions for one day. Then, heat curing was applied. For curing conditions, previous studies have been used. Aygörmez et al. [35] used three temperatures (80, 60, 40 °C) and three different times (72, 24, 2 h) for geopolymer production. The most appropriate curing temperature and time were found to be 72 h at 60 °C. Taking advantage of this situation, the samples were kept at 60 °C for 72 h in this study. Samples were placed in the oven with a fireproof oven bag. The main benefit of this situation is preventing water evaporation in the internal structure and thus ensures the continuation of the reaction. Post-curing samples were stored at ambient conditions as far as the test day. The series of Rilem sand, recycled waste concrete sand, river sand, sandstone, silica sand, and basalt sand series are shown with RS, RWC, RVS, SDS, SS, and BS, respectively.

Table 4
Geopolymer mixing quantities (g).

Metakaolin	Sand	Slag	NaOH (12 M)	Na_2SiO_3
450.0	1012.5	60.0	150.0	300.0

7, 28, and 56 days of UPV, compressive, and flexural strength values of the produced samples were found. The cube samples (50 × 50 × 50 mm) were used for the compressive strength test according to ASTM C109 [36]. Similarly, the prism samples (40 × 40 × 160 mm) were used for the flexural strength test according to ASTM C348 [37]. Three samples were used for each test. The figures show the results of all three samples for each test. In all figures, sample numbers for three samples in each test are indicated by numbers (1, 2, and 3). Besides, unit weight, water absorption, and voids ratio values were found using cube samples. In addition, the workability results of geopolymer samples were also found. In order to determine the abrasion resistance, cube samples (71 × 71 × 71 mm) were subjected to the abrasion test in accordance with EN 7138 [38] for all series. A high-temperature test was performed at temperatures of 200, 400, 600, and 800 °C. Pre-test samples were kept for 24 h at 105 °C. The rate of increase per minute of the high-temperature furnace was set to 5 °C/min. The samples were kept at a constant temperature for 1 h when they reached the target temperature. Then the samples were left to cool in the oven with the oven lid open. 180 cycles were applied for the freezing-thawing test. 1 cycle involves keeping samples at −18 °C for 12 h and +4 °C for 12 h. Compressive strength, flexural strength, weight changes, and UPV were studied both before and after the freezing-thawing test and high-temperature test. Freezing-thawing and high-temperature tests were applied after the 56th day. Visual examination for the samples was made after the tests. Also, SEM and XRD analyses were made for microstructure analysis.

3. Results and discussion

3.1. Strength results

Compressive and flexural strength results produced by using six different sand types are given in Figs. 1 and 2. According to the results, it was found that the highest results were obtained using

basalt sand in terms of both flexural strength and compressive strength. Its 28-day average compressive strength was 67.8 MPa, while its average flexural strength was 10.9 MPa. The main reason for this situation is that basalt is denser, more durable, and less water absorbent. Also, increasing the workability with the addition of basalt sand is another reason that increases the strength. The low cost and abundant basalt aggregate pave the way for it to be an economical product providing high strength. These results showed that the aggregate type and amount have an important effect on capillary water absorption. The minimum water absorption and voids ratio were observed in the basalt sand added sample. The dense structure formed by the addition of basalt sand also reduces the penetration of water. Thus, the basalt sand added sample, which had a less porous structure, was found to have higher strength [39–41].

When the strength properties were examined, it was observed that the silica sand added geopolymer samples also had high strength. After 56 days, 66.2 MPa of average compressive strength and 9.8 MPa of average flexural strength were obtained. Silica sand reduces water absorption rates like basalt sand. It also has a positive effect on cohesion. Also, it has been found to contribute to geopolymerization due to its high SiO_2 ratio. The dissolution of the sand surface and increasing the polysiloxo (-Si-O-) combination contributes to the geopolymerization by binding it to the geopolymer gel. Due to this situation, it has strengthened the metakaolin based geopolymer. This reinforcement is optimal up to 100 μm. It is difficult to bind to the geopolymer gel if larger particles (200–240 μm) are used. This is because the combination formation is nanometers and large particles are insufficient to combine. Due to this situation, all sand types were added to the mixture using a 100 μm sieve in this study. It contributes to the strengthening of the bonds by contributing to the production of Si-Al gel. Besides, by creating a strong interface between the matrix and the aggregate, it serves as a buffer against cracks. It also contributes to the reduction of the pore structure [42,43]. Sandstone, which makes up about 40% of the sedimentary rocks in the world, is found in large amounts in the earth's crust. The efficient use of sandstone in geopolymer samples will save a significant amount of natural resources, creating a sustainable effect. Besides, the cost of sandstone produced by the quarry is also very low. In this study, the strength of sandstone increased due to the reaction caused by the high quartz content in the metakaolin used as a binder material. After 56 days, 62.8 MPa of average compressive strength and 9.3 MPa of average flexural strength were obtained. Similar to silica and basalt sand, the fact that sandstones reduce the water absorption and voids ratio significantly is one of the reasons which increases the strength [44]. In the case of river sand, the strength values were lower than basalt, silica and sandstone added samples. Due to the river sand being round, the crack length is longer and more, while the water absorption and voids ratio are higher. These situations decrease strength properties [45]. With the use of Rilem sand, the strength properties decreased compared to other sands. The main reason for this situation is that Rilem sand acts as an inert fine aggregate in geopolymerization and does not participate in the reaction. Thus, the resulting strength properties were formed only due to metakaolin and slag [46]. The average compressive strength results of 56.2 MPa and 58.4 MPa were obtained at the end of 56 days while 8.7 MPa and 9.1 MPa of average flexural strength results were obtained with Rilem sand and river sand, respectively.

In the case of using waste concrete aggregate, a decrease in compressive strength was observed. These results are consistent with the results of Portland cement concretes. Waste concrete aggregates have lower strengths than traditional concrete. Aggregate and paste interfaces are weaker than new traditional concrete. Flexural strength results also behaved similarly to compressive strength results. Nevertheless, thanks to its calcium hydroxide and other calcium products, the waste concrete aggregate has contributed to the progression of the reactions in the interface transition region. In the geopolymer sample produced with waste concrete aggregate, 34.4 MPa of average compressive strength, and 5.3 MPa of average flexural strength were obtained after 56 days. It has been observed that it is suitable for use in terms of environmental protection and sustainability as well as obtaining acceptable results for structural concrete elements [47,48].

In the study, strength results on three different days were examined. When the results were examined, an increase was observed in the 28-day results compared to the 7-day results, while a decrease in 56-day results was determined compared to 28-day results. The main condition that constitutes this situation is due to the application of high temperature for curing. The application of high-temperature curing contributes significantly to early strength. The high temperature quickly promotes the dissolution of solid binder materials and the formation of reaction products. It

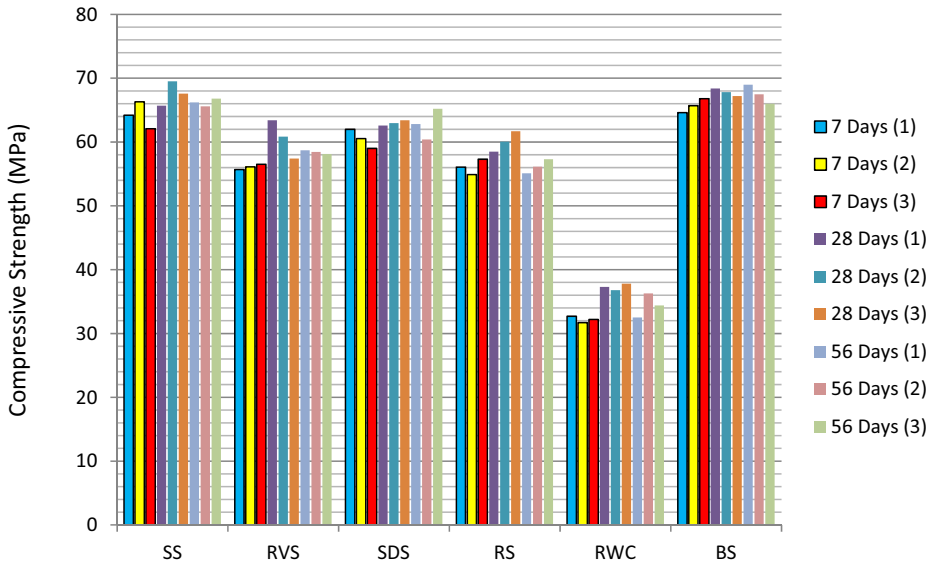


Fig. 1. The mixes' compressive strength values.

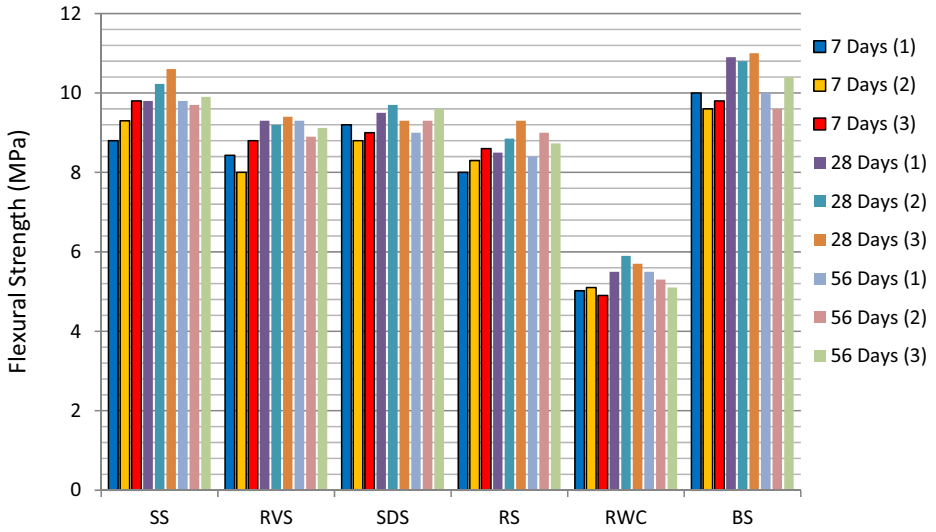


Fig. 2. The mixes' flexural strength values.

Table 5
The physical properties results.

	Unit weight (g/cm^3)	Water absorption (%)	Voids ratio (%)	Flow (mm)
SS	2.44	7.76	24.42	215
RVS	2.39	8.19	25	197
SDS	2.44	7.97	24.65	208
RS	2.39	8.33	25.2	189
RWC	2.35	9.47	31.6	162
BS	2.48	7.39	24.31	222

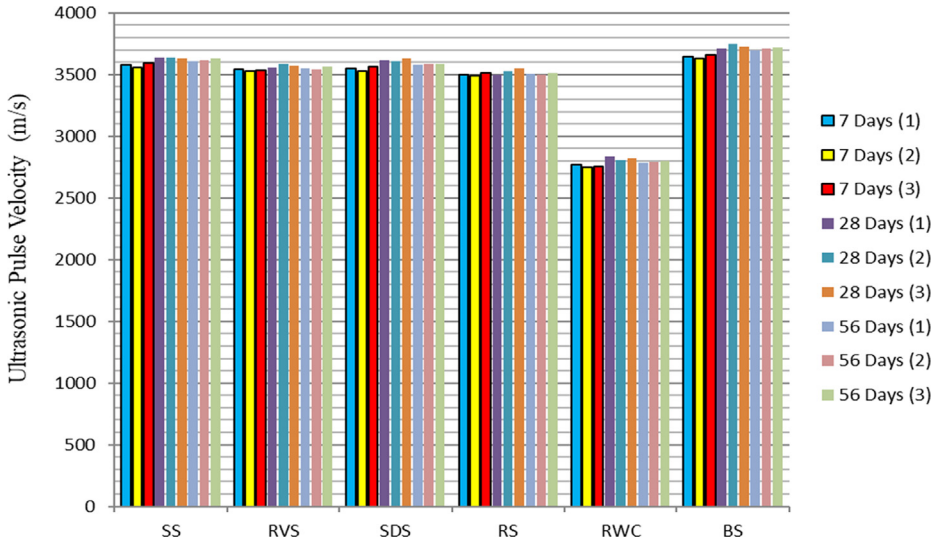


Fig. 3. The mixes' UPV values.

has been determined that the heat energy with the optimum temperature controls the geopolymerization reaction and strength development. However, the rapid reaction occurring starts to have negative effects on microstructure and reaction products. Puertas et al. [49] stated that the important parameter determining the geopolymerization rate is diffusion, while the reaction products will be collected close to the binder material particles. However, in the future, the homogeneity of the microstructure starts to deteriorate and the continuous reactions decrease. If the situation is explained in more detail, the dissolution of the binder materials, ie reactive species, will accelerate with increased temperature. A more dense and heterogeneous microstructure is formed after reactive intensive processing. In this way, more reaction products are formed. The dense structure leads to a delay in reactions in the future, while diffusion becomes difficult. With the effect of this situation, decreases started to appear after the strength increases up to 28 days. However, it was seen that the reductions were limited. Aygörmez et al. [52] showed that the decrease lost its initial speed after 28 days regarding heat curing. It was observed that the results obtained at the end of the 1 year were close to the

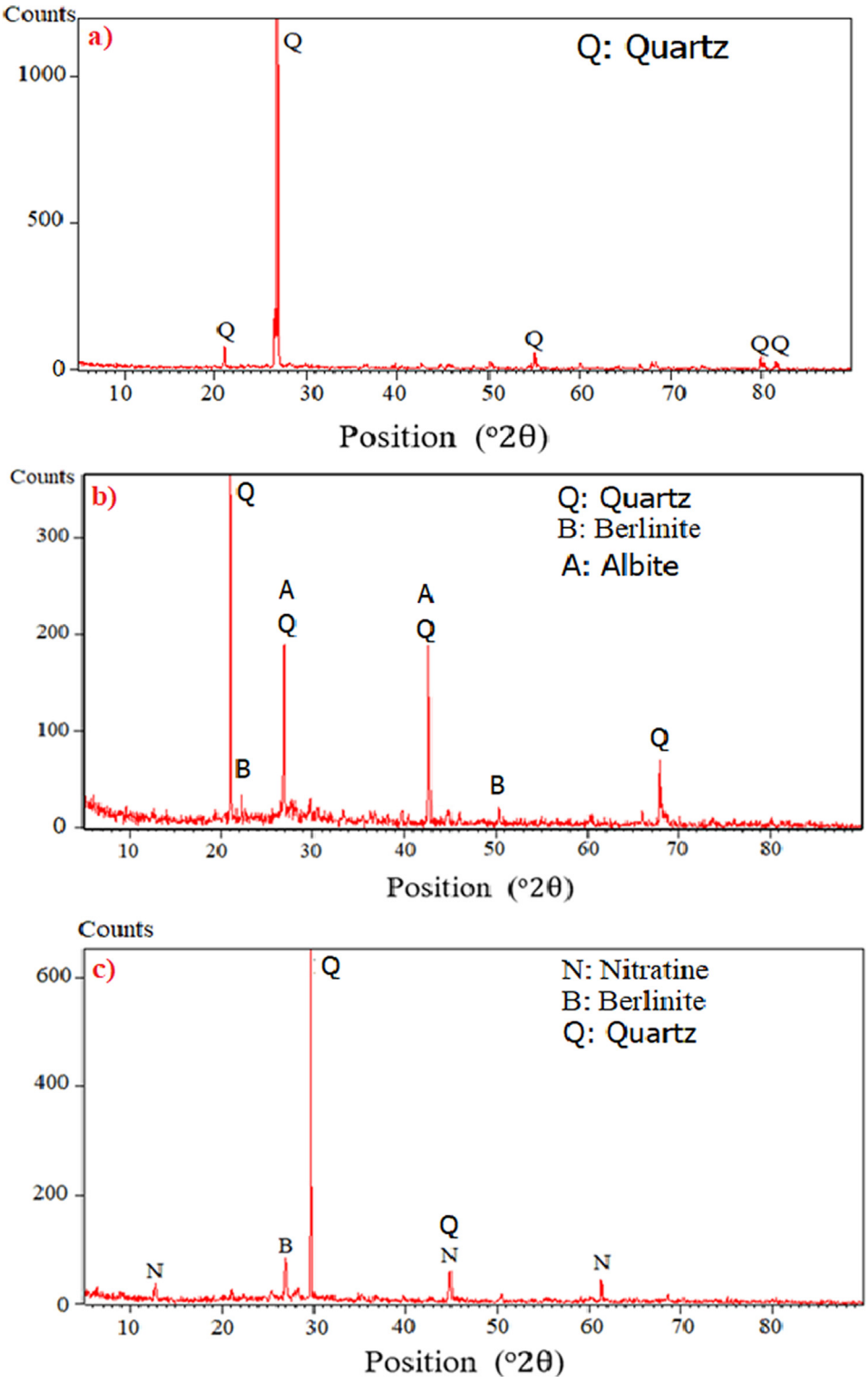


Fig. 4. XRD patterns of samples a) SS b) RVS c) SDS.

results obtained in 90 days. This is because of the compact structure of the geopolymer matrix. According to these results, it shows that gel chemistry is effective in the long-term behavior of geopolymers. The results are seen to be compatible with the literature [50–52].

3.2. Physical properties and ultrasonic pulse velocity results

Unit weight, water absorption, voids ratio, and workability properties were found to examine the physical properties of the geopolymer matrix. The results are given in Table 5. The difference

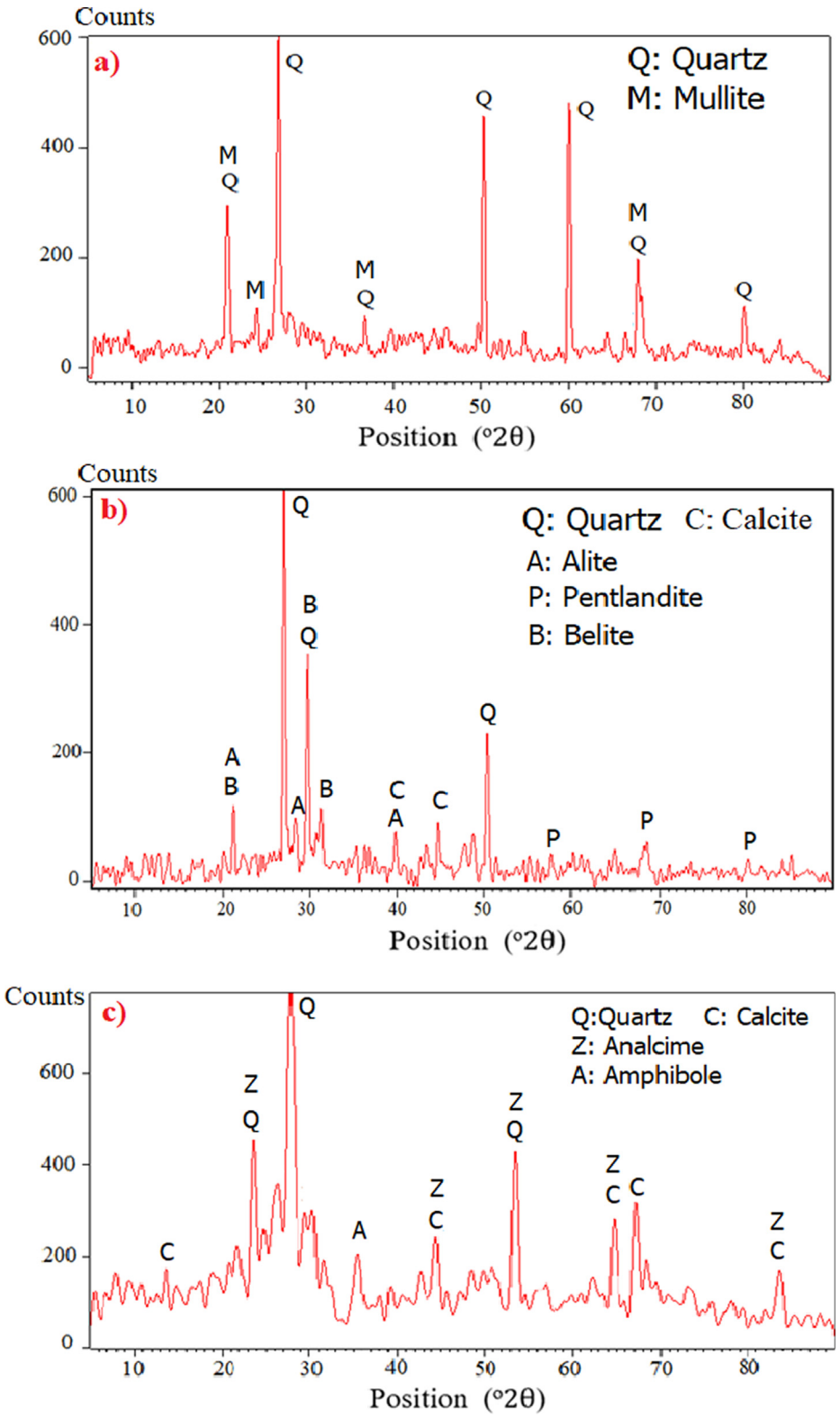


Fig. 5. XRD patterns of samples a) RS b) RWC c) BS.

between the results depends on the type of sand used. When the results were analyzed, the unit weight increase also brought about a decrease in the voids ratio and water absorption rate [32]. Basalt sand has a very dense structure and has increased unit weight. While the highest unit weight was in basalt sand added geopolymer sample, the lowest water absorption and voids ratio were also observed. In this way, it is also seen that the fine aggregate's type and amount have an important effect on the behavior of capillary water absorption [40,41]. Similarly, silica sand and sandstone added samples had a low water absorption and voids ratio as well as high unit weights [42,44]. In river sand and Rilem sand added sample, it was observed that the unit weight decreased, while

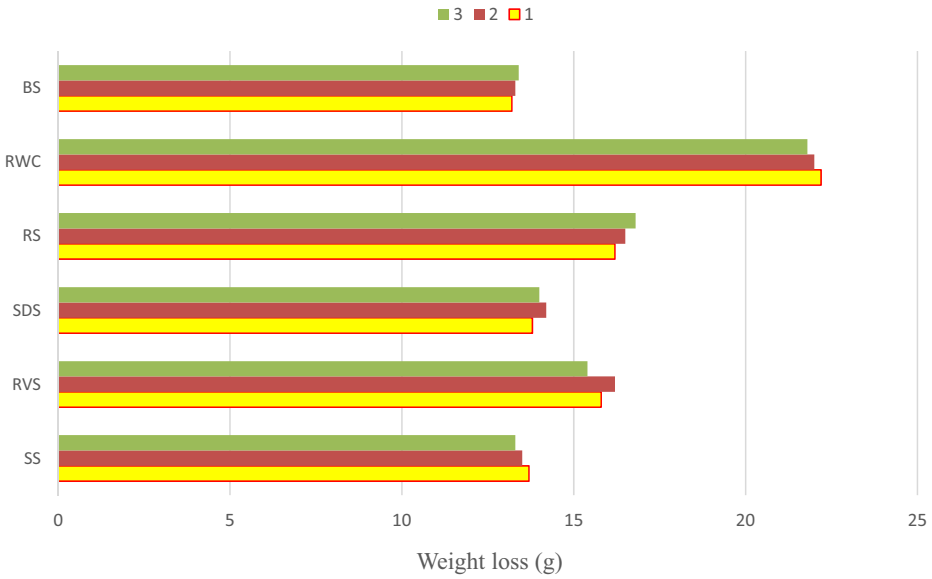


Fig. 6. Weight loss due to abrasion.

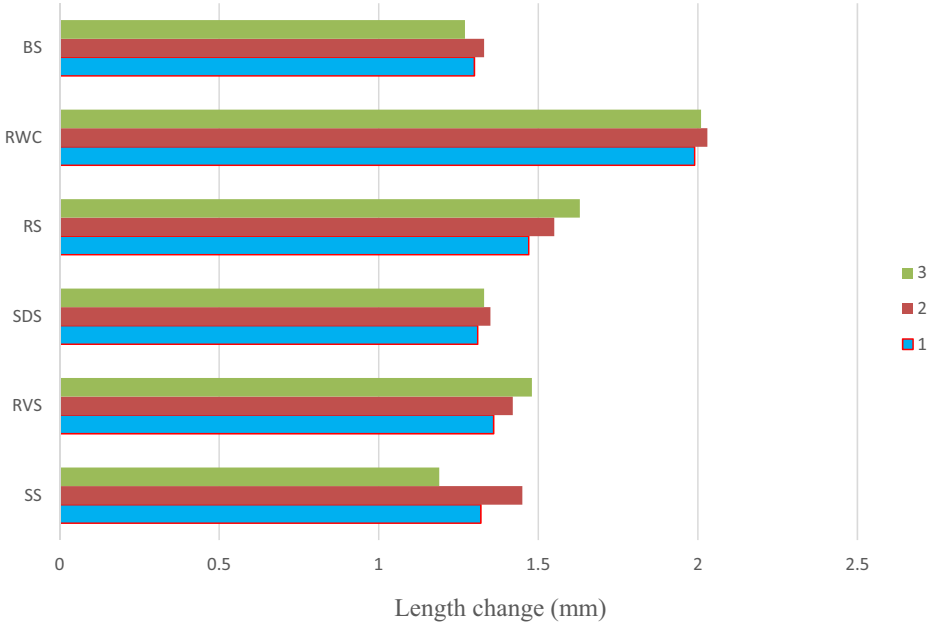


Fig. 7. Length change due to abrasion.

the rate of water absorption and void increased inversely. The lowest unit weight was observed in the geopolymer samples with waste concrete aggregate, while the highest water absorption and voids ratio were observed. The main reason for this situation is that the mortars connected to waste concrete aggregates have high porosity and act as a potential channel for water transport in matrices [47,48]. The slump flow values of the geopolymer fresh mortar samples produced in the study were determined by measuring the average diameter. When the workability values of the geopolymer mortar samples were examined, it was seen that the highest result was in the series using basalt sand, while the lowest result was in the series using waste concrete aggregate. It is seen that the results obtained are in parallel with the strength results.

UPV tests were conducted to investigate the continuity of the geopolymeric matrix and the effect of using different sands. 7, 28, and 56 days of ultrasonic pulse velocity values of the six series produced are shown in Fig. 3. There is an inverse proportion between the wave velocity and the increase in the voids number for the material. Also, it was observed that there is a specific relationship between the wave velocity and the unit weight for the material. The penetration rate is determined by calculating the period it takes for the sound waves to travel from the source point to the receiver, taking into account the distance traveled [32,40]. Since the increase in the number of voids in the matrix structure will also increase the time to go, the ultrasonic sound penetration rate coefficient will decrease. The voids ratio is an important factor for determining the mechanical properties of hardened mortar and concrete. While the highest ultrasonic pulse velocity values were obtained in the basalt sand added sample with the lowest voids ratio in the six samples examined, the lowest UPV values were

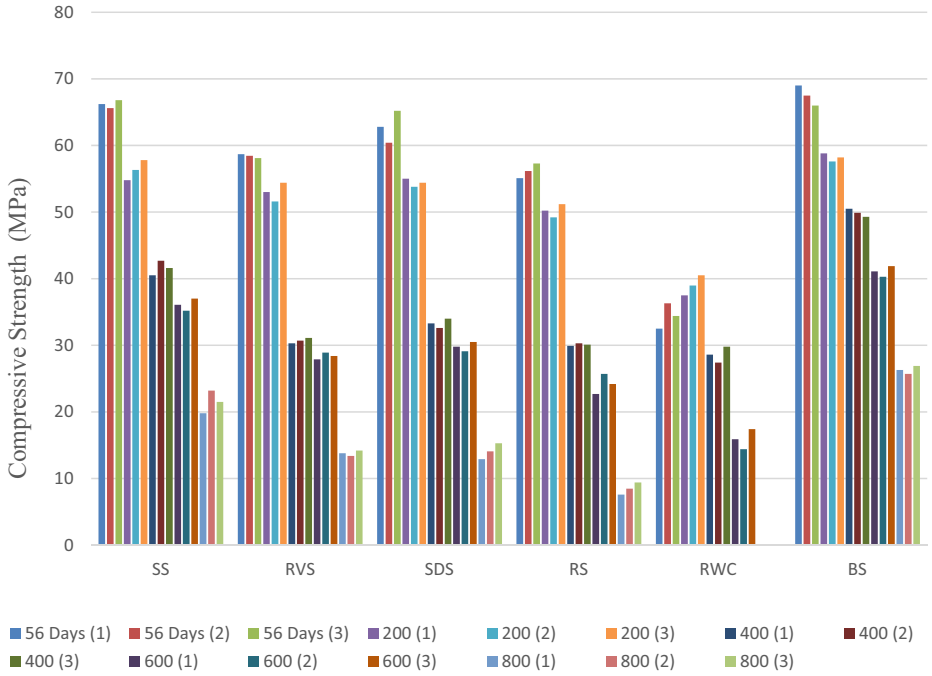


Fig. 8. Residual compressive strengths.

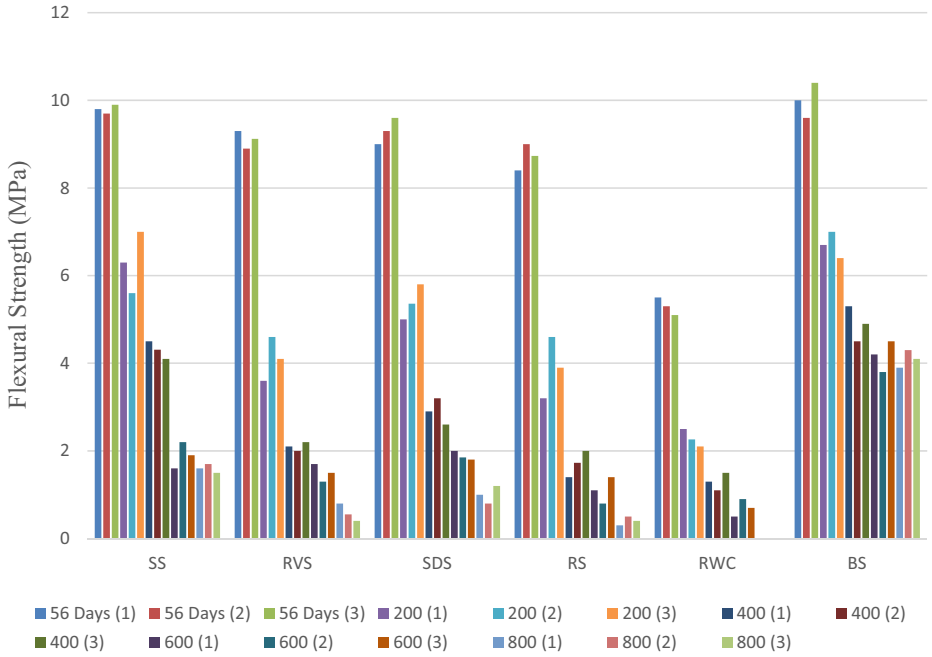


Fig. 9. Residual flexural strengths.

observed in the waste concrete aggregate added sample with the highest voids ratio. In the basalt sand added sample, 3711 m/s of average UPV value was obtained after 56 days, while in the waste concrete aggregate added sample, 2792 m/s of average UPV value was obtained after 56 days. When the ultrasonic pulse velocity results on three different days were examined, firstly an increase was observed similarly, then some decrease was seen. This is because the homogeneity deteriorates in the future and causes an increase in the number of voids [50,51]. While the average value of 3644 m/s in the basalt sand added sample increased to 3730 m/s at the end of 28 days, it decreased slightly to 5611 m/s after 56 days. Similarly, in the sample with waste concrete aggregate, the average value which was 2758 m/s at the end of 7 days increased to 2821 m/s at the end of 28 days and decreased to 2792 m/s at the end of 56 days.

3.3. XRD patterns

XRD patterns were examined for six different series produced in this study. XRD patterns for six series are given in Figs. 4 and 5. The presence of quartz was detected in the peaks for all series. The major reason is the presence of highly crystalline silica in the

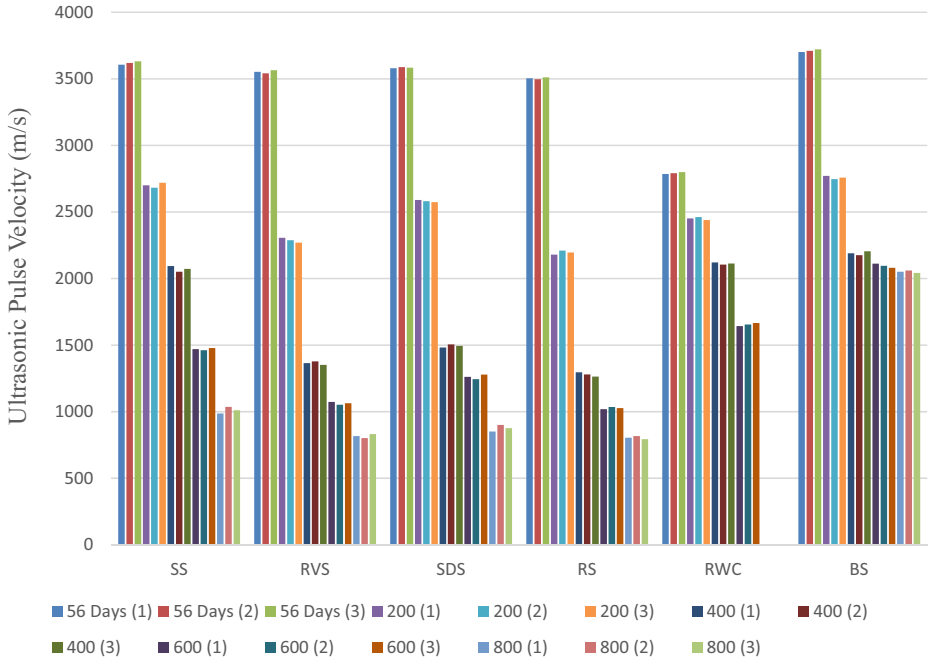


Fig. 10. Residual UPV values.

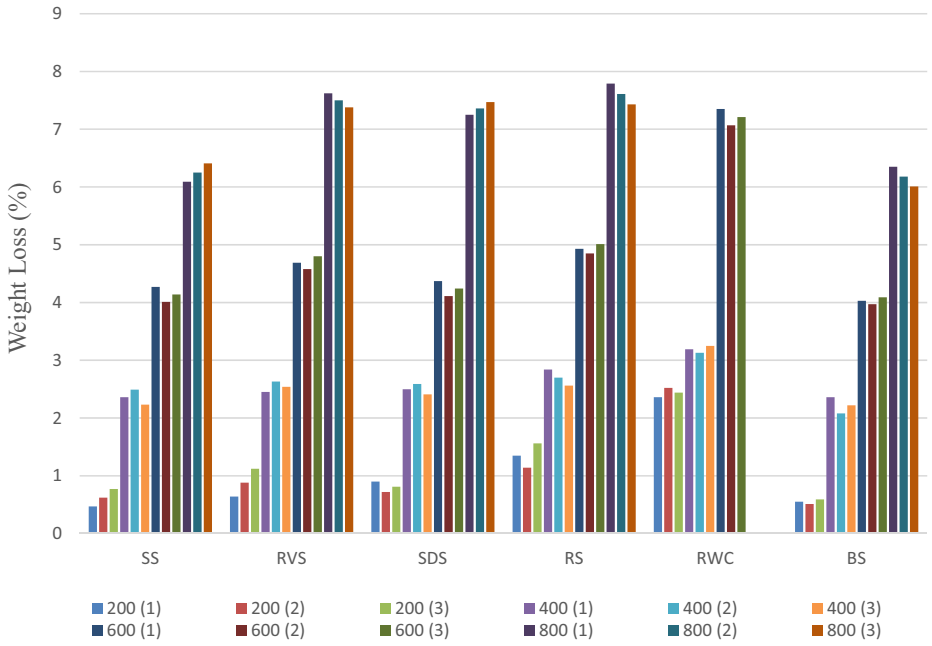


Fig. 11. Weight-loss results.

metakaolin binder material. In river sand added samples, albite and berlinite were also detected besides quartz. Nitratine and berlinite were detected in the samples with sandstone. Mullite was detected in Rilem sand added samples as well as a high rate of quartz. High levels of belite, alite, and calcite were detected in the waste concrete aggregate added samples. This situation arose from Portland Cement used in waste concrete aggregate. In basalt sand added samples, besides quartz, analcime, amphibole, and calcite were detected. The presence of analcime ($NaAlSi_2O_6{\cdot}H_2O$) and amphibole ($NaCa_2(Mg,Fe,Al)_5(Al,Si)_8O_{22}(OH)_2$) together with calcite ($CaCO_3$) indicates the formation of sodium aluminate chemical bonds which has (Si-O-Al) chemical structure. Polymerization continued with the penetration of the Na^+ cation into the Si-O-Al chemical structure. In this way, it was observed that geopolymerization was strengthened and strength values increased. The presence of peaks between 20° and 30° 2θ in all series studied is a sign of satisfactory geopolymerization. Higher compressive strengths of the mixtures confirm microstructural analysis on the formation of geopolymer phases in manufactured mixtures [53].

3.4. Abrasion resistance

Abrasion is a significant durability problem in mortars and concrete. The length change and weight loss results after the test for

six series with three samples are given in Figs. 6 and 7. When the results were analyzed in general, the lowest average weight loss was in the basalt sand added sample (13.2 g), while the highest average weight loss was in the waste concrete aggregate added sample (22 g). The lowest average length change was in the basalt sand added sample as 1.3 mm, while the highest average length change was in the waste concrete aggregate added sample as 2.01 mm. High abrasion resistance in basalt sand added specimens could be clarified by its hard structure [40]. It was also observed that there was a close relationship between the abrasion resistance and capillary water absorption rates. In another interview, higher abrasion was observed with higher rates of capillary water absorption [32]. Samples with waste concrete aggregates had higher abrasion values due to higher water absorption rates [47]. Due to this situation, it has been observed that the durability of basalt, silica sand, and sandstone added samples increased. The results trend is parallel to the strength results.

3.5. High-temperature test

Comparison of the 56-day results of the six series with the compressive strength, flexural strength, UPV values at the end of 200, 400, 600, and 800 °C of temperatures are given in Figs. 8–10. The weight-loss results are given in Fig. 11. When the results were examined, there were decreases in mechanical properties. The main reason for the decrease in strength results is the free water evaporation and dehydration in the matrix with the thermal reaction mechanism formed after 500 °C temperature [52–54]. These decreases started to increase after 600 °C. To better explain the loss of strength after 500 °C, the concept of steam effect should be used. The main reason for the loss of strength caused by increasing high temperatures is the steam effect. The water in the matrix structure turns into steam with the temperature. The temperature rises above 100 °C continuously increase the internal pressure. After the limit at which the vapor pressure can be maximum, the matrix condenses with less permeability. Resistance decreases against thermal effects created in this way. This situation creates thermal cracks on the surfaces. Evaporation of water in the matrix structure also causes mass loss. Cracks formed by the effect of thermal shrinkage lead to loss of strength as well as mass loss. Besides, high temperatures create thermal incompatibility by creating microcracks in the interface transition region between the paste and the aggregate [55]. Besides, the aluminosilicate gel structure undergoes more crystallization at higher temperatures. This situation leads to the thermochemical decomposition of crystal lattices at the end of the crystallization stress caused by increasing temperature. With the recrystallization process, ductility and strength are negatively affected. This inhomogeneous condition creates thermal incompatibility. This is another phenomenon that triggers the formation of micro-cracks.



Fig. 12. Geopolymer samples after 800 °C.

Against these effects, the stronger the structure of the geopolymer sample, the more quickly it radiates heat and is exposed to less thermal gradients. This situation limits thermal cracks and fragmentation. Besides, flexural strength results are significantly affected by microstructural defects caused by the cracks' spread and the growth of porous structures after high temperatures [56]. When the test results were analyzed, it was found that similar behavior was observed before the test. The highest strength results were obtained after the test in basalt sand added samples. Average compressive strengths of basalt sand added samples after temperatures of 200,400, 600, and 800 °C were 58.2 MPa, 49.9 MPa, 41.1 MPa, and 26.3 MPa, respectively. Again in basalt sand added samples, average flexural strengths after temperatures of 200,400, 600, and 800 °C were 6.7 MPa, 4.9 MPa, 4.2 MPa, and 4.1 MPa, respectively. In basalt sand added samples, a higher thermal conductivity occurs because the density is higher. Due to its thermal stability, negligible deformations occur while weight loss and thermal reactions are less [57]. Besides, basalt sands produce a natural nucleator such as Fe_3O_4 during the melting of basalt rocks, contributing to the formation of a resistant microstructure and having a high residual strength after 800 °C [32].

In waste concrete aggregate added samples, a behavior similar was observed to the high-temperature behavior of the conventional concrete. In traditional concretes, after 200–300 °C temperature, compressive strength increase can be seen. As a result of the 200 °C of temperature effect, the strength increase was observed, then this situation was replaced by a decrease in waste concrete aggregate added samples. After an 800 °C temperature effect, it was observed that the waste concrete aggregate added sample lost its stability similar to the Portland cement sample [58]. Average compressive strengths in the waste concrete aggregate added sample after temperatures of 200,400 and 600 °C were 39.0 MPa, 28.6 MPa, and 15.9 MPa, respectively. Again, the average flexural strengths of waste concrete aggregate samples after temperatures of 200, 400, and 600 °C were 2.3 MPa, 1.3 MPa, and 0.7 MPa, respectively. Since a dense structure was formed after the use of silica sand and sandstone, the residual strengths were also high. Besides, the contribution of silica sand to geopolymerization thanks to SiO_2 is another important reason that increases the resistance [42]. Apart from waste concrete aggregate added samples, it was found that geopolymer samples maintained their compact structure.

When the ultrasonic pulse velocity results were examined after the tests, decreases were seen similar to the strength results. Significant decreases were observed after 300 °C. The damage to the solid matrix of the samples triggered this situation. The temperature increase also increases the water evaporation and growth in the pore structure occurs. This triggers mass loss. The water loss in the matrix also creates additional gaps. The increase in the gaps

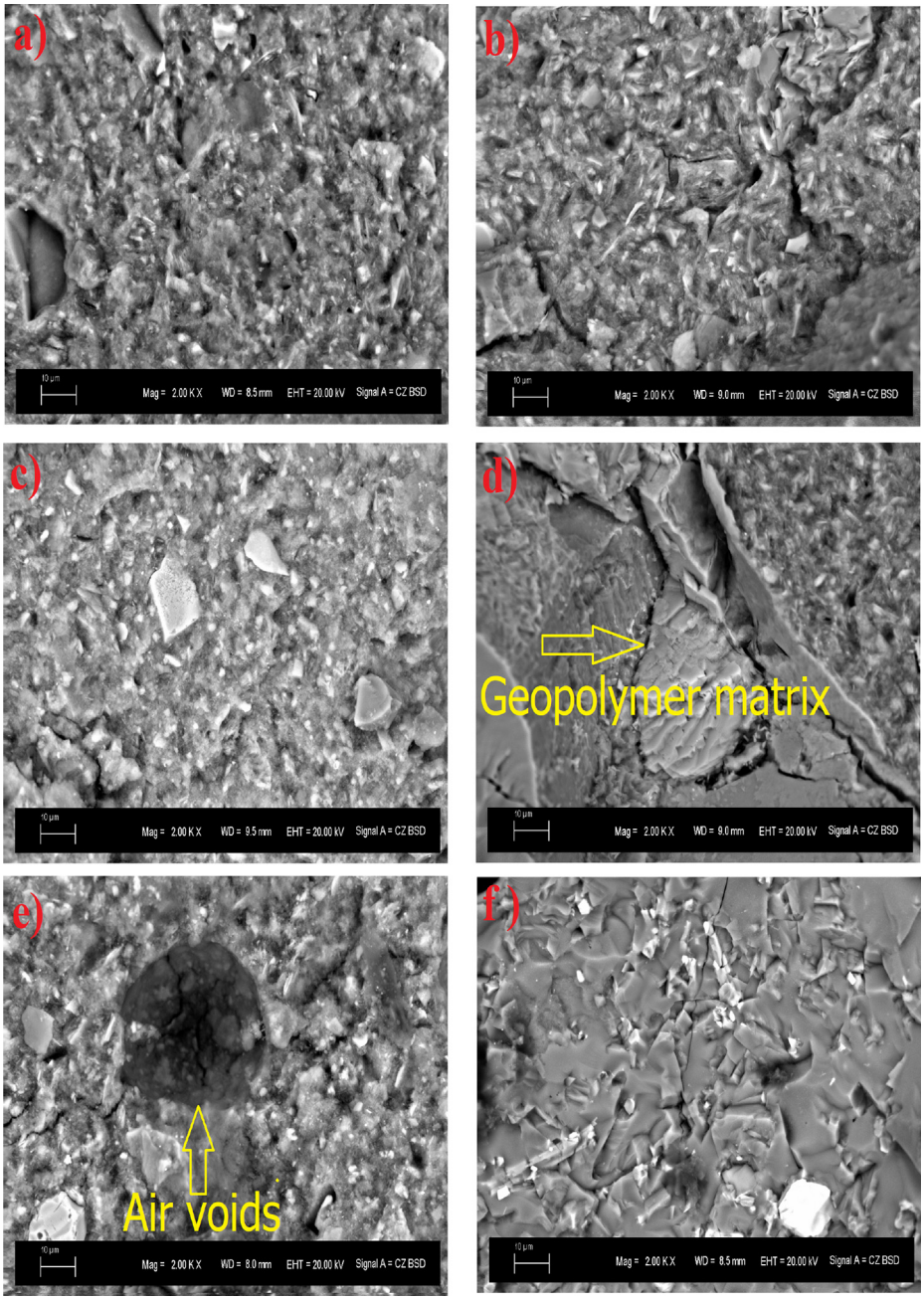


Fig. 13. SEM micrographs for samples a) SS b) RVS c) SDS d) RS e) RWC f) BS.

increases the time it takes for the ultrasonic speed waves to propagate while causing a decrease in UPV values. Besides, the decrease in the density of the sample structure due to micro-cracks increasing with temperature caused a decrease in UPV values [59]. While the highest UPV values were formed in the densest basalt sand added sample, the results could not be taken since the waste concrete aggregate added samples were dispersed after 800 °C. In basalt sand added samples, average UPV values after temperatures of 200,400, 600 and 800 °C were 2759 m/s, 2190 m/s, 2096 m/s and 2051 m/s, respectively.

There was an increase in weight losses after high temperature. While the temperature accelerates the dehydration mechanism in the matrix structure, it enables the existing moisture to move to the outer surface. This situation causes weight loss in the internal structure and microstructure. Weight loss can be examined in three stages. Physically absorbed water loss is between 30 and 210 °C, while polymer side chains deteriorate between 210 and 400 °C. Between 400 and 500 °C, disruptions begin to occur in the main polymer chains. As a result of these stages, weight loss increases continuously. Also, distortions in aggregate-matrix interface with high temperatures increase weight loss [60–62]. Considering all these situations, the lowest weight losses were observed in basalt sand added samples, while the highest weight losses were observed in waste concrete aggregate added samples. The average weight losses in basalt sand added samples after 200,400, 600 and 800 °C temperatures were 0.55%, 2.22%, 4.03%, and 6.18%, respectively. The average weight losses in the waste concrete aggregate added samples after temperatures of 200,400, 600 °C were 2.44%, 3.19%, and 7.21%, respectively.

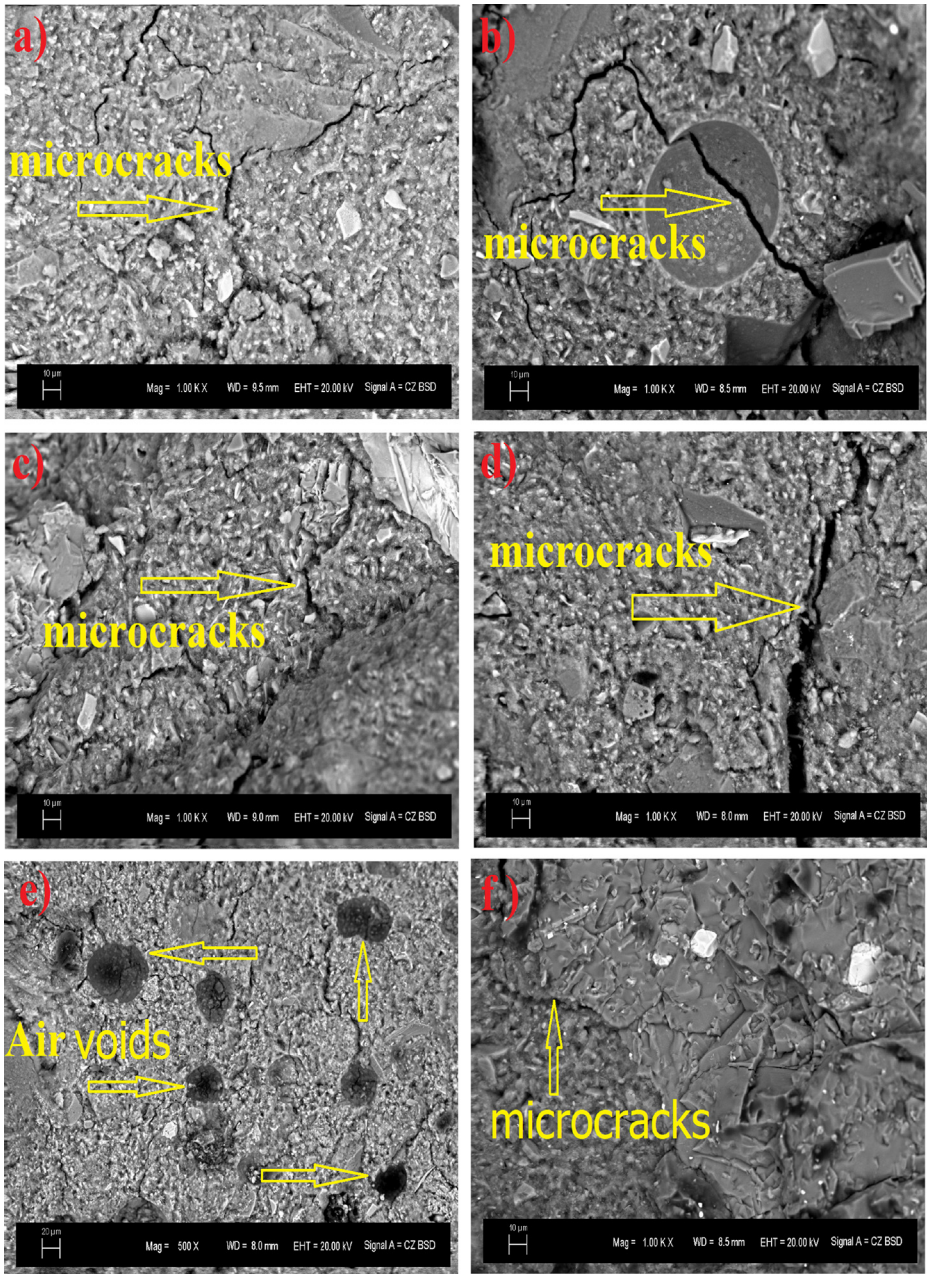


Fig. 14. SEM micrographs for samples a) SS b) RVS c) SDS d) RS e) RWC f) BS after 600 °C.

Surface changes on the samples after high temperature were investigated and given in Fig. 12. Photos were taken immediately after samples were taken out of the oven after testing. After the temperature of 800 °C, except for waste concrete aggregate added samples, the surface cracks remained limited while significant color changes began to appear. This is in line with the fact that geopolymer samples maintain their stability against high temperature [32]. While a slightly brittle structure was formed in the samples, some tendency to become rough on the surfaces started. The major reason is that the main chains in the geopolymer matrix can be damaged due to temperature. In the waste concrete aggregate added sample, dispersion occurred after 800 °C temperature. This situation arose from the use of waste concrete as aggregate.

In this study, the microstructures of composite products were investigated to see the effect of different sands. Fig. 13 shows pre-high temperature SEM micrographs and Fig. 14 shows post-high temperature SEM micrographs. In SEM micrographs, the bond structure between the geopolymer matrix and the aggregate was examined. Parallels with compressive strength results were observed in the micrographs studied. When micrographs of samples using basalt sand, silica sand, and sandstone were examined, a dense matrix structure was observed. Similarly, the degree of homogeneity was found to be good in geopolymeric matrices. In the case of using Rilem sand and river sand, some micro-cracks have been formed. In the case of using waste concrete aggregate, the presence of air bubbles was determined. This situation shows that in the case of using waste concrete aggregate, the geopolymer matrix-aggregate interface bond is weak. This reduces the degree of attachment [53].

SEM micrographs of six samples after 600 °C were examined to see the sample structure after high temperature. It was observed that micro-cracks started to progress according to the pre-high

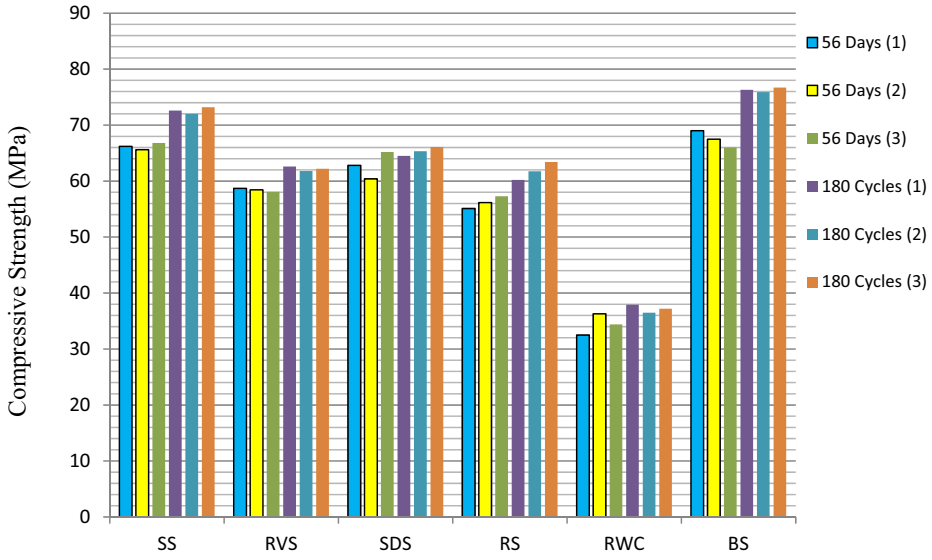


Fig. 15. Compressive strengths with the freezing-thawing effect.

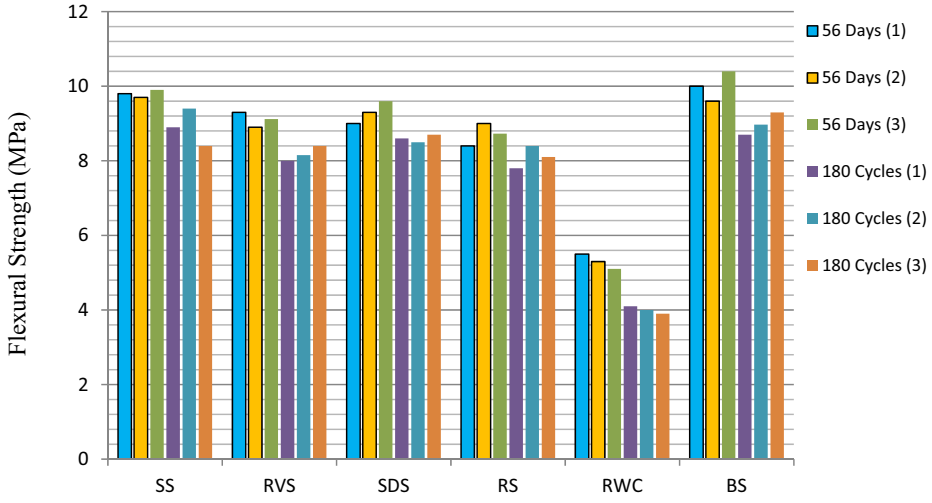


Fig. 16. Flexural strengths with the freezing-thawing effect.

temperature situation. However, micro-cracks were limited in samples prepared using dense basalt sand, silica sand, and sandstone. In the case of river sand and Rilem sand, it was observed that the cracks increased a little more, but the general stable structure was preserved. It was observed that in the samples with waste concrete aggregate, air bubbles began to form with the progression of microcracks. The main reasons for this situation are weight loss, matrix decomposition, and phase transformations. These conditions cause structural defects and then intensify the formation of defects. In this way, the structure has become more porous. This progressive situation caused the dispersion of the sample after 800 °C temperature. However, in other sand types, it has been observed that the classical metakaolin-based geopolymer samples maintained their stability [32].

3.6. Freezing-thawing test

Comparison of strengths and UPV results obtained from the 180 cycles of freeze–thaw test with 56-day results are given in Figs. 15–17. Likewise, the weight change resulting from the test is given in Fig. 18. When the compressive strength results at the end of the test were examined, an increase was observed although a decrease was expected. The main reason that creates this remarkable situation is that the moist environment in the experimental environment fills the sample voids. Geopolymer matrices have a compact structure and good adhesion degree, making them resistant to the freeze–thaw effect. Besides, freeze–thaw cycles create progress in matrices. In this way, the production of geopolymeric products continues after 180 cycles. This situation can be considered as a continuation of the curing process of the geopolymer. Compressive strength and UPV results were also higher due to this situation. In this regard, it has been reported by different authors that freezing-thawing tests have positive effects on concrete properties (strength and dynamic modulus) under wet and humid conditions [34,63–64]. According to these, it was observed that binder materials such as slag, metakaolin, and fly ash were activated during the test, and frost attack was prevented thanks to the formation of binding products. When the flexural strength results were investigated, a decrease was seen in contrast to the compressive strength results. When the samples are subjected to compressive load, cracks occur parallel to the compressive load. Damage consists of bending stress perpendicular to the compressive load. Thus,

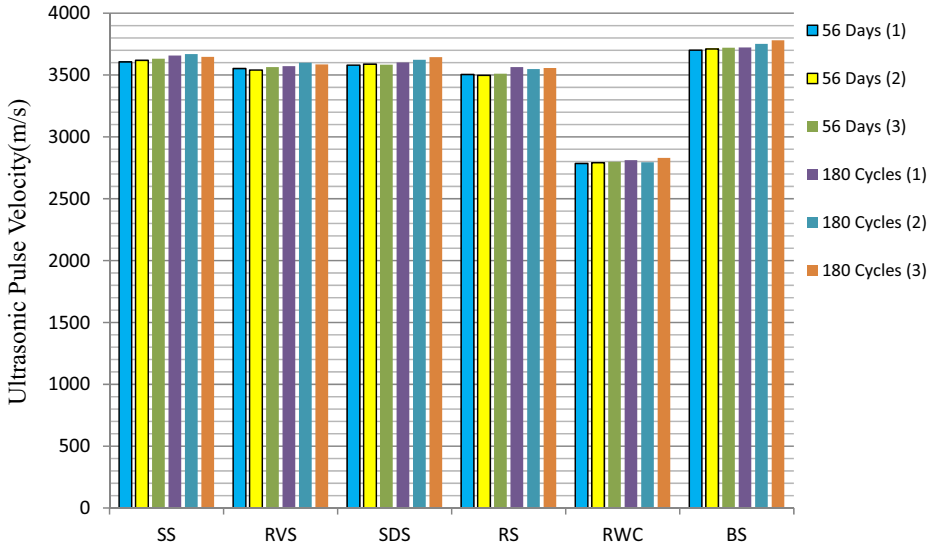


Fig. 17. Ultrasonic pulse velocity results with the freezing-thawing effect.

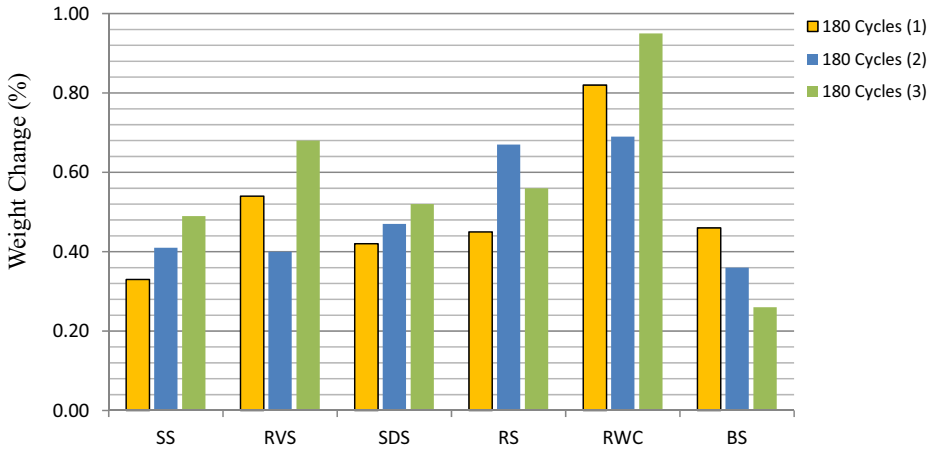


Fig. 18. Weight change rates after 180 cycles.



Fig. 19. Geopolymer samples with the freezing-thawing test.

freeze–thaw cycles are more effective for flexural strength according to compressive strength. The different sands used in this study play an important role in strengthening the aggregate-paste interface. In the basalt sand added sample, the aggregate-paste interface was strengthened and the highest compressive strength and UPV values were obtained. The lowest values were obtained in the waste concrete aggregate added sample. The results were similar to before testing. In the basalt sand added sample, 76.3 MPa of average compressive strength, 9.0 MPa of average flexural strength, and 3752 m/s of average ultrasonic pulse velocity results were obtained at the end of the test. At the end of the test, 37.2 MPa of average compressive strength, 4.1 MPa of average flexural strength, and 2812 m/s of average ultrasonic pulse velocity results were obtained in the waste concrete aggregate added sample. These results showed that it is acceptable to use waste concrete aggregates for structural elements.

When the weight changes at the end of freeze–thaw were examined, increases were observed. At the end of the test, the gaps formed due to micro-cracks in the samples are quickly filled with the humid environment effect. The weight change that occurs during freeze–thaw cycles results from the movement of the moist medium into and out of the sample and microcracks. This caused an increase in weight here. However, these increases were observed to be limited [65]. At the same time, this caused an

increase in UPV values as it will also decrease the transition time of ultrasonic waves. If basalt sand is used here, the weight increase is lower since a denser structure will be formed. The hard and compact structure limits weight gain. The weight increase in waste concrete aggregate added samples was higher. When the average weight increases were examined, it was observed that they were between 0.36% and 0.82%.

After the freeze–thaw test consisting of 180 cycles, the samples were examined visually. According to the visual inspection after the test, no important damage was observed. While there was no significant damage in the outer appearance, it was observed that the micro cracks formed in the internal structure were positively reflected on the strength effect since they were filled with the moist environment effect. It was also observed that microcracks were not at a level to cause crack formation on the outer surface. Therefore, it has been seen that the samples show high resistance against the freeze–thaw effect [66–67]. The visual view of the samples after 300 cycles is given in Fig. 19.

4. Conclusions

For this paper, mechanical and durability properties of metakaolin-based geopolymer samples prepared by using six different aggregates were examined and related results were found:

- When the strength and UPV results of 7.28 and 56 days were analyzed, an increase was seen in the results from 7 days to 28 days, and then a decrease was observed from 28 days to 56 days. The main reason is the use of high temperature for curing. While high-temperature application provides an early high strength of the samples, in the following periods, the homogeneity of the microstructure has caused disruptions and a decrease in the continuous reaction, resulting in some decrease in the results. But these declines have been limited.
- The type of sand used was decisive to rank the mechanical properties. The highest performance in mechanical properties has been observed as the workability increased and a more dense and durable and less water absorbent structure was formed with the use of basalt sand. In the case of using silica sand, the SiO_2 ratio increased and contributed to geopolymerization. This has led to high results. In the case of using sandstone, significant increases in mechanical properties were observed thanks to the high CaO ratio and high dense structure. In the case of river sand and Rilem sand, relatively lower results compared to others, but high results were obtained. In the case of using waste concrete aggregate, the lowest results were obtained. The fact that the properties of the waste concrete aggregate are lower than the conventional concrete and the aggregate-paste interface is weak. However, the results were still acceptable. In mechanical tests and abrasion tests, better results were obtained in sandy samples with denser structure and lower capillary water absorption and porosity values.
- A significant reduction in mechanical properties was observed after the high-temperature test. Similar to the situation before the high-temperature test, high results were obtained in samples using basalt sand. The thermal conductivity of the dense structure of the basalt sand allowed the sample to remain thermally stable. It has been observed that geopolymer samples maintained their stability after 800 °C temperature, excluding the waste concrete aggregate. In the case of using waste concrete aggregate, dispersion occurred similar to Portland Cement. The results were also compatible with SEM images.
- After the freeze–thaw test, UPV and compressive strength values increased instead of decreasing. This has been caused by the continuation of geopolymerization with the moist environment effect where the freeze–thaw test is applied. Very low increases in weight have occurred. Geopolymer samples showed significant resistance to freeze–thaw tests thanks to their compact structure.

Declaration of Competing Interest

The authors declare that they have no known competing financial interests or personal relationships that could have appeared to influence the work reported in this paper.

Acknowledgment

This work was supported by the research fund of the Yildiz Technical University, the authors would like to express their sincere gratitude to the scientific research coordination unit for their financial support to the project (Project number: FBA-2019-3558).

References

[1] E. Prudhomme, P. Michaud, E. Joussein, S. Rossignol, Influence of raw materials and potassium and silicon concentrations on the formation of a zeolite phase in a geopolymer network during thermal treatment, J. Non-Cryst. Solids 358 (16) (2012) 1908–1916.
[2] H. Wang, H. Li, F. Yan, Synthesis and mechanical properties of metakaolinite-based geopolymer, Colloids Surf. A: Physicochem. Eng. Asp. 268 (2005) 1–6.
[3] H. Tchakoute Kouamo, A. Elimbi, J.A. Mbey, C.J. Ngally Sabouang, D. Njopwouo, Constr. Build. Mater. 35 (2012) 960–969.
[4] M. Uysal, M.M. Al-mashhadani, Y. Aygörmez, O. Canpolat, Effect of using colemanite waste and silica fume as partial replacement on the performance of metakaolin-based geopolymer mortars, Constr. Build. Mater. 176 (2018) 271–282.
[5] P.L. Maier, S.A. Durham, Beneficial use of recycled materials in concrete mixtures, Constr. Build. Mater. 29 (2012) 428–437.
[6] S. Marinković, J. Dragaš, I. Ignjatović, N. Tošić, Environmental assessment of green concretes for structural use, J. Clean. Prod. 154 (2017) 633–649.
[7] F. Faleschini, M.A. Zanini, C. Pellegrino, S. Pasinato, Sustainable management and supply of natural and recycled aggregates in a medium-size integrated plant, Waste Manage. 49 (2016) 146–155.
[8] G. Dobbelaere, J. de Brito, L. Evangelista, Definition of an equivalent functional unit for structural concrete incorporating recycled aggregates, Eng. Struct. 122 (2016) 196–208.
[9] A.A.M. Amer, K. Ezziane, A. Bougara, M.H. Adjoudj, Rheological and mechanical behavior of concrete made with pre-saturated and dried recycled concrete aggregates, Constr. Build. Mater. 123 (2016) 300–308.
[10] M. Etxeberria, E. Vázquez, A. Marí, M. Barra, Influence of the amount of recycled coarse aggregates and production process on properties of recycled aggregate concrete, Cem. Concr. Res. 37 (5) (2007) 735–742.
[11] K.K. Sagoe-Crentsil, T. Brown, A.H. Taylor, Performance of concrete made with commercially produced coarse recycled concrete aggregate, Cem. Concr. Res. 31 (5) (2001) 707–712.
[12] S.W. Tabsh, A.S. Abdelfatah, Influence of recycled concrete aggregates on strength properties of concrete, Constr. Build. Mater. 23 (2009) 1163–1167.
[13] S. Marinković, V. Radonjanin, M. Malešev, I. Ignjatović, Comparative environmental assessment of natural and recycled aggregate concrete, Waste Manage. 30 (11) (2010) 2255–2264.
[14] M. Sánchez, P.A. Gutiérrez, Study on the influence of attached mortar content on the properties of recycled concrete aggregate, Constr. Build. Mater. 23 (2009) 872–877.
[15] F. Debieb, L. Courard, S. Kenai, R. Degeimbre, Mechanical and durability properties of concrete using contaminated recycled aggregates, Cem. Concr. Compos. 32 (6) (2010) 421–426.
[16] V. Tam, X.F. Gao, C.M. Tam, Microstructural analysis of recycled aggregate concrete produced from two-stage mixing approach, Cem. Concr. Res. 35 (6) (2005) 1195–1203.
[17] A. Akbarnezhad et al., Effects of the parent concrete properties and crushing procedure on the properties of coarse recycled concrete aggregates, J. Mater. Civ. Eng. 25 (12) (2013) 1795–1802.
[18] A. Akbarnezhad, Z.S.M. Nadoushani, A computational method for selection of optimal concrete recycling strategy, Mag. Concr. Res. 67 (11) (2015) 543–558.
[19] D. Constantiner, S. Diamond, Alkali release from feldspars into pore solutions, Cem. Concr. Res. 33 (4) (2003) 549–554.
[20] H.M. Al-Baijat, The use of basalt aggregates in concrete mixes in Jordan, Jordan J. Civ. Eng. 2 (1) (2008) 63–70.
[21] M. Uysal, K. Yilmaz, Effect of mineral admixtures on properties of self-compacting concrete, Cem. Concr. Compos. 33 (2011) 771–776.
[22] L. Laibao, Z. Yunsheng, Z. Wenhua, L. Zhiyong, Z. Lihua, Investigating the influence of basalt as mineral admixture on hydration and microstructure formation mechanism of cement, Constr. Build. Mater. 48 (2013) 434–440.

[23] M.E.S. Saraya, Study the pozzolanic activity of fresh basalt, J. Mater. Sci. Eng 1 (2011) 40–50.
[24] H. Maiah, G. Al-Khateeb, Effect of basalt and limestone aggregate combinations on Superpave aggregate properties, The 5th Jordanian International Civil Engineering Conference, At Amman, Jordan.
[25] A. Sudhahar, D.L. Venkateshbabu, K. Sridevi, An investigation on the usefulness of extracted-dolomite-silica fine in concretes, International Conference on Sustainability Challenges and Advances in Concrete Technology, 2012.
[26] A. Vishnumanohar, Performance of normal concrete with eco sand (Finely Graded Silica) as fine aggregate, Int J. Eng. Invasion 3 (5) (2014).
[27] J.R. Mackechnie, Shrinkage of concrete containing graywacke sandstone aggregate, ACI Mater. J. 103 (2004) 390–396.
[28] M. Yılmaz, A. Tugrul, The effects of different sandstone aggregates on concrete strength, Constr. Build. Mater. 35 (2012) 294–303.
[29] E. Rahmathulla Noufal, U. Manju, I-sand: an environment friendly alternative to river sand in Reinforced Cement Concrete constructions, Constr. Build. Mater. 125 (2016) 1152–1157.
[30] H.Y. Zhang, V. Kodur, S.L. Qi, L. Cao, B. Wu, Development of metakaolin-fly ash based geopolymers for fire resistance applications, Constr. Build. Mater. 55 (2014) 38–45.
[31] P. Duan, C. Yan, W. Zhou, Compressive strength and microstructure of fly ash based geopolymer blended with silica fume under thermal cycle, Cem. Concr. Compos. 78 (2017) 108–119.
[32] A. Celik, K. Yilmaz, O. Canpolat, M.M. Al-mashhadani, Y. Aygörmez, M. Uysal, High-temperature behavior and mechanical characteristics of boron waste additive metakaolin based geopolymer composites reinforced with synthetic fibers, Constr. Build. Mater. 187 (2018) 1190–1203.
[33] L. Cai, H. Wang, Y. Fu, Freeze-thaw resistance of alkali-slag concrete based on response surface methodology, Constr. Build. Mater. 49 (2013) 70–76.
[34] Z. Yunsheng, S. Wei, L. Zongjin, Z. Xiangming, C. Chungkong, Impact properties of geopolymer based extrudates incorporated with fly ash and PVA short fiber, Constr. Build. Mater. 22 (3) (2008) 370–383.
[35] Y. Aygörmez, O. Canpolat, M. Uysal, M.M. Al-mashhadani, Compressive and flexural strength behaviors of metakaolin based geopolymer mortars manufactured by different procedures, in: 4th International Conference on Green Design and Manufacture IConGDM 2030 (2018).
[36] ASTM C109/109M, Standard Test Method for Compressive Strength of Hydraulic Cement Mortars (Using 2-in. or [50-mm] Cube Specimens) 1. Chemical Analysis, (C109/C109M – 11b), (2010) pp. 1–9.
[37] ASTM C348, Standard Test Method for Flexural Strength of Hydraulic-Cement Mortars ASTM C348. Annual Book of ASTM Standards, 4, (1998) pp. 2–7.
[38] European Standard, EN 1338, Concrete paving blocks – requirements and test, methods (2003).
[39] H. Binici, Effect of crushed ceramic and basaltic pumice as fine aggregates on concrete mortars properties, Constr. Build. Mater. 21 (6) (2007) 1191–1197.
[40] H. Binici, O. Aksogan, Durability of concrete made with natural granular granite, silica sand and powders of waste marble and basalt as fine aggregate, J. Build. Eng. 19 (2018) 109–121.
[41] I.S. Kishore, L. Mounika, C.M. Prasad, B.H. Krishna, Experimental study on the use of basalt aggregate in concrete mixes, SSRG Int. J. Civ. Eng. 2 (4) (2015) 37–40.
[42] M. Steinerova, Mechanical properties of geopolymer mortars in relation to their porous structure, Ceram. -Silikáty 55 (4) (2011) 362–372.
[43] X. Li, F. Rao, S. Song, M.A. Corona-Arroyo, N. Ortiz-Lara, E.A. Aguilar-Reyes, Effects of aggregates on the mechanical properties and microstructure of geothermal metakaolin-based geopolymers, Results Phys. 11 (2018) 267–273.
[44] S. Kumar, B.S. Thomas, V. Gupta, P. Basu, S. Shrivastava, Sandstone wastes as aggregate and its usefulness in cement concrete–a comprehensive review, Renew. Sustain. Energy Rev. 81 (2018) 1147–1153.
[45] M. Bederina, Z. Makhloufi, A. Bounoua, T. Bouziani, M. Quéneudec, Effect of partial and total replacement of siliceous river sand with limestone crushed sand on the durability of mortars exposed to chemical solutions, Constr. Build. Mater. 47 (2013) 146–158.
[46] J. Dong, C. Li, H. Liu, L. Zhang, J. Liu, Investigating the mechanical property and reaction mechanism of geopolymers cement with red Pisha Sandstone, Constr. Build. Mater. 201 (2019) 641–650.
[47] P. Nuaklong, V. Sata, P. Chindaprasirt, Influence of recycled aggregate on fly ash geopolymer concrete properties, J. Cleaner Prod. 112 (2016) 2300–2307.
[48] K. Rahal, Mechanical properties of concrete with recycled coarse aggregate, Build. Environ. 42 (2007) 407–415.
[49] F. Puertas, S. Marfınez-Ramírez, S. Alonso, T. Vázquez, Alkali-activated fly ash/slag cements: Strength behaviour and hydration products, Cem. Concr. Res. 30 (10) (2000) 1625–1632.
[50] Z. Sun, A. Vollpracht, One year geopolymerisation of sodium silicate activated fly ash and metakaolin geopolymers, Cem. Concr. Compos. 95 (2019) 98–110.
[51] P. Sukmak, S. Horpibulsuk, S.-L. Shen, Strength development in clay–fly ash geopolymer, Constr. Build. Mater. 40 (2013) 566–574.
[52] Y. Aygörmez, O. Canpolat, M.M. Al-mashhadani, A survey on one year strength performance of reinforced geopolymer composites, Constr. Build. Mater. 264 (2020) 120267.
[53] N. Ali, O. Canpolat, Y. Aygörmez, M.M. Al-Mashhadani, Evaluation of the 12–24 mm basalt fibers and boron waste on reinforced metakaolin-based geopolymer, Constr. Build. Mater. 251 (2020) 118976.
[54] Y. Aygörmez, O. Canpolat, M.M. Al-mashhadani, M. Uysal, Elevated temperature, freezing-thawing and wetting-drying effects on polypropylene fiber reinforced metakaolin based geopolymer composites, Constr. Build. Mater. 235 (2020) 117502.
[55] X. Jiang, R. Xiao, M. Zhang, W. Hu, Y. Bai, B. Huang, A laboratory investigation of steel to fly ash-based geopolymer paste bonding behavior after exposure to elevated temperatures, Constr. Build. Mater. 254 (2020) 119267.
[56] H.Y. Zhang, V. Kodur, B. Wu, L. Cao, Qi S. Liang, Comparative thermal and mechanical performance of geopolymers derived from metakaolin and fly ash, J. Mater. Civ. Eng. 28 (2) (2016) 1–12.
[57] J. Strzałkowski, H. Garbalińska, The Influence of Silica Fume on the Mechanical and Thermal Parameters of Portland Cement Concretes, J. Ecol. Eng. 20 (9) (2019).
[58] P. Nuaklong, P. Jongvivatsakul, T. Pothisiri, V. Sata, P. Chindaprasirt, Influence of rice husk ash on mechanical properties and fire resistance of recycled aggregate high-calcium fly ash geopolymer concrete, J. Cleaner Prod. 252 (2020) 119797.
[59] I.B. Topçu, C. Karakurt, Properties of reinforced concrete steel rebars exposed to high temperatures, Adv. Mater. Sci. Eng. 2008 (2001).
[60] D.L.Y. Kong, J.G. Sanjayan, K.S. Crentsil, Comparative performance of geopolymers made with metakaolin and fly ash after exposure to elevated temperatures, Cem. Concr. Res. 37 (2007) 1583–1589.
[61] G. Masi, W.D. Rickard, M.C. Bignozzi, A. Van Riessen, The effect of organic and inorganic fibres on the mechanical and thermal properties of aluminate activated geopolymers, Compos. B Eng. 76 (2015) 218–228.
[62] P. He, D. Jia, T. Lin, M. Wang, Y. Zhou, Effects of high-temperature heat treatment on the mechanical properties of unidirectional carbon fiber reinforced geopolymer composites, Ceram. Int. 36 (2010) 1447–1453.
[63] F. Puertas, T. Amat, A. Fernández-Jiménez, T. Vázquez, Mechanical and durable behaviour of alkaline cement mortars reinforced with polypropylene fibres, Cem. Concr. Res. 33 (12) (2003) 2031–2036.
[64] O. Bortnovsky, K. Dvořáková, P. Roubíček, J. Boušek, Ž. Průdková, P. Baxa, Development, properties, and production of geopolymers based on secondary raw materials, in: 3rd Int. Conf. on Alkali Activated Materials Research, Production and Utilization, 2007, pp. 83–96.
[65] P. Sun, H.C. Wu, Chemical and freeze-thaw resistance of fly ash-based inorganic mortars, Fuel 111 (2013) 740–745.
[66] A.A. Arslan, M. Uysal, A. Yılmaz, M.M. Al-mashhadani, O. Canpolat, F. Şahin, Y. Aygörmez, Influence of wetting-drying curing system on the performance of fiber reinforced metakaolin-based geopolymer composites, Constr. Build. Mater. 225 (2019) 909–926.
[67] Y. Aygörmez, O. Canpolat, M.M. Al-mashhadani, Assessment of geopolymer composites durability at one year age, J. Build. Eng. (2020) 101453.